Journal of Biomechanics 191 (2025) 112920

Contents lists available at ScienceDirect

Journal of Biomechanics

journal homepage: www.elsevier.com/locate/jbiomech

Gait classification in individuals with unilateral transfemoral amputation using random forest and k-means clustering

Yufan He [a], Mingyu Hu [a], Alpha C.H. Lai [a], Mark W.P. Koh [a], Hiroaki Hobara [b], Fan Gao [c], Toshiki Kobayashi [d,*]

[a] Department of Biomedical Engineering, Faculty of Engineering, The Hong Kong Polytechnic University, Hong Kong, China
[b] Faculty of Advanced Engineering, Tokyo University of Science, Tokyo, Japan
[c] Department of Kinesiology and Health Promotion, University of Kentucky, Lexington, KY, USA
[d] Orthocare Innovations, Edmonds, WA, USA

ARTICLE INFO

Keywords:
Amputee
Gait pattern
Walk
Symmetry
Machine learning

ABSTRACT

Cluster analysis has been recently applied to categorize gait patterns in individuals with unilateral transfemoral amputation (uTFA). However, conventional clustering methods largely rely on experiential knowledge of gait analysis, lacking a scientific foundation for feature selection. The aim of this study was to investigate if gait patterns could be classified using random forest and k-means clustering in individuals with uTFA. Spatiotemporal data and vertical ground reaction force (vGRF) were collected using an instrumented treadmill from twelve individuals with uTFA and twelve age-matched non-disabled individuals participated. Absolute symmetry index (ASI) was obtained and normalized. These parameters served as inputs for a random forest model to assess their importance. K-means clustering was applied to determine the optimal number of clusters according to Silhouette Score and the Elbow Method. Differences in demographic, spatiotemporal, and ASI parameters among clusters were assessed using One-way ANOVA and independent-sample Kruskal-Wallis tests. Random forest model revealed that swing phase and single limb support duration time symmetries were most significant for distinguishing individuals with uTFA from non-disabled. The k-means identified three distinct clusters: cluster 1 exhibited the lowest symmetry with the shortest prosthetic single limb support duration; cluster 2 displayed the highest symmetry with the longest prosthetic single limb support duration and intact step length; cluster 3 demonstrated moderate symmetry with the highest cadence. This study highlights that customized rehabilitation targeting specific gait patterns—such as strengthening muscles to increase single-limb support and step length, and modulating cadence—could enhance gait performance in individuals with uTFA.

1. Introduction

Individuals with unilateral transfemoral amputation (uTFA) exhibit asymmetric gait pattern during walking due to partial loss of the lower limb and muscles on the amputated side (Winiarski et al., 2021). This gait asymmetry is related to multiple factors such as walking speed (Nolan et al., 2003), type of prosthetic components (Kaufman et al., 2012; Petersen et al., 2010; Schaarschmidt et al., 2012), level of amputation (Keklicek et al., 2019), muscle strength (Heitzmann et al., 2020; Krajbich et al., 2023; Rutkowska-Kucharska et al., 2018), compensatory patterns (Harandi et al., 2020), amputation surgery (Ranz et al., 2017), and person-dependent gait deviations. Additionally, residual femur length (Bell et al., 2013), cardiorespiratory fitness (Gjovaag et al., 2014), prosthetic socket type (Traballesi et al., 2011), prosthetic alignment (Kobayashi et al., 2013; Zhang et al., 2019), and the individual's walking habits also affect the spatiotemporal parameters of gait. Classifying gait deviations is essential for identifying compensatory patterns and tailoring rehabilitation programs aimed at improving gait symmetry and function. It also enables objective tracking of patients' progress and aids in optimizing prosthetic interventions. However, due to the multifaceted nature of these factors, it is challenging to holistically classify gait in individuals with uTFA.

Limited studies have been conducted to categorize gait in individuals with uTFA (Ichimura et al., 2022). One study successfully identified three distinct gait clusters among individuals with uTFA using an unsupervised machine learning approach—clustering—with each cluster

* Corresponding author at: Orthocare Innovations, 123 2nd Ave South, Edmonds, WA 98020, USA.
E-mail address: tkobayashi@orthocareinnovations.com (T. Kobayashi).

https://doi.org/10.1016/j.jbiomech.2025.112920
Accepted 17 August 2025
Available online 18 August 2025

showing significant differences in cadence and step length across various walking speeds (Ichimura et al., 2022). Utilizing an unsupervised machine learning approach is advantageous because it bypasses the need to consider all factors affecting gait, relying instead on direct data-driven pattern recognition to classify gait patterns. This approach has been successfully applied to identify distinct gait patterns in other patient populations, such as those with stroke or cerebral palsy, providing a means of tracking and evaluation of gait variations over time (Abbasi et al., 2021; Chantraine et al., 2022; Roche et al., 2014). Conventional classifiers that incorporate both kinematic and electromyographic (EMG) data can distinguish gait phases with high accuracy (Mobarak et al., 2024; Tigrini et al., 2024), offering valuable insights for gait phases recognition in smart prostheses. Integrating such classifiers with gait data for individuals with uTFA could further improve locomotion and accelerate the development of intelligent prosthetic technologies. However, studies specifically focused on gait pattern classification in individuals with uTFA remain limited. By applying clustering techniques to gait data from this population, our study aims to objectively classify distinct gait types and ultimately inform personalized interventions that address specific gait deviations and rehabilitation needs.

However, using only a clustering algorithm has its limitation, as it does not reveal which specific gait features contribute most to gait classification. Typically, researchers select key features for model training based on their expertise in gait analysis. While expert input is valuable, relying solely on subjective judgement can reduce objectivity and reproducibility in feature selection, potentially limiting the generalizability of the findings. The random forest model can be utilized to calculate feature importance, aiding in identification of the most critical characteristics that distinguish between groups (Luo et al., 2020). By training the model on gait data from both able-bodied individuals and those with uTFA, it can assess which features most effectively differentiate these groups. Features that significantly contribute to the model's classification accuracy are ranked higher, indicating their importance in capturing the unique aspects of each group's gait pattern.

Symmetry parameters are metrics used to quantify the degree of bilateral symmetry, typically calculated from measured bilateral kinematic or kinetic gait parameters (Viteckova et al., 2018). Different formulas can yield various values, generally represented as percentages within a range, such as 0 to 1, where 0 indicates perfect symmetry and 1 indicates complete asymmetry. For individuals with uTFA, bilateral asymmetry is common (Schaarschmidt et al., 2012), and symmetry parameters could serve as valuable indicators for assessing gait quality and monitoring improvement over time.

In this study, the first objective is to assess the importance of the features (include kinematic parameters, spatiotemporal parameters, and symmetry parameters derived from the spatiotemporal parameters) that distinguish the gait of individuals with uTFA from that of non-disabled using a random forest model. These features are then used to cluster individuals with uTFA. The second objective is to identify the gait patterns of different clusters. Our hypothesis is that the clustering algorithm can identify multiple distinct gait patterns with significant differences in spatiotemporal and symmetry parameters.

2. Methods

2.1. Participants

Twelve uTFA individuals (ten male and two female individuals; age: 54 ± 7 years; time since amputation: 18.2 ± 16.5 years; body height: 1.74 ± 0.07 m; body mass: 74.4 ± 15.4 kg; BMI: 24.5 ± 4.5 kg/m2; residual limb length: 22.1 ± 5.2 cm; walking speed: 1.78 ± 0.38 km/h) participated in this study (Table 1). The inclusion criteria were: 1) at least 18 years old, 2) uTFA, 3) ability to walk on a treadmill without using assistive devices (e.g., crutch, walker), and 4) no neuromusculoskeletal complications other than amputation. An age-matched control group of twelve able-bodied individuals (nine male and three female individuals; age: 54 ± 7 years; body height: 1.66 ± 0.09 m; body mass: 66.8 ± 10.4 kg; BMI: 24.2 ± 2.1 kg/m2; walking speed: 2.33 ± 0.20 km/h) was also recruited. This study was approved by the Human Subjects Ethics Sub-Committee of the Hong Kong Polytechnic University (number: HSEARS20220719001). All participants were informed of the contents of the study, and consent was obtained before participation.

2.2. Protocol

The experimental setting is shown in Fig. 1. A Zebris FDM-T treadmill (Zebris Medical GmbH, Germany) was used to collect spatiotemporal gait parameters, including walking speed, cadence, step length, stride length, step width, step time, duration time of gait phases (stance phase, loading response, single limb support, double limb support, preswing phase, and swing phase), as well as vGRFs for both the left and right limbs. The test–retest reliability and validity of Zebris had been well established in previous studies conducted with healthy participants (Reed et al., 2013; Van Alsenoy et al., 2019). All individuals were asked to warm up on the treadmill for a minimum of 5 min (Zeni Jr and Higginson, 2010). They were encouraged to walk without aids, but the handrails were available for support if needed. All individuals walked on the treadmill for two trials, each lasting for one minute at a self-selected speed, which was determined by gradually increasing the treadmill

Table 1
Demographic information of individuals with unilateral transfemoral amputation.

Participants	Gender	Amputation side	Type of PK	K-level	Reason for amputation	Age (year)	Time since amputation (year)	Body height (m)	Body mass (kg)	BMI	Residual limb length (cm)	Walking speed (km/h)
1	M	L	Mauch	4	Infection	52	6	1.76	78	25.2	20	1.79
2	M	L	Paso	3	Trauma	43	7	1.74	100	33.0	24.5	1.40
3	F	L	3R106 PRO	3	Trauma	56	7	1.75	93	30.4	15	1.71
4	M	L	3R80	4	Cancer	54	34	1.85	71	20.8	27.8	1.21
5	M	L	RHEO	4	Trauma	66	53	1.79	71	22.2	17.4	2.82
6	M	R	TSA	4	Trauma	62	45	1.78	65	20.5	23	2.01
7	M	L	Paso	3	Cancer	57	7	1.77	65	20.8	19.5	1.81
8	M	L	Covered	4	Trauma	48	27	1.69	68	23.8	30	1.73
9	F	R	KX06	4	Trauma	55	5	1.56	53	21.8	23	1.70
10	M	R	Paso	4	Trauma	49	11	1.76	74	23.9	15	2.11
11	M	L	Jiguang	4	Trauma	44	4	1.78	101	31.9	31	1.50
12	M	L	3R78	4	Infection	61	12	1.63	54	20.3	18.5	1.71

Abbreviations: PK: prosthetic knee; BMI: body mass index; CT: control; M: male; F: female; R: right; L: left; TSA: traditional single axis. Prosthetic knee: Mauch knee, Paso knee, and RHEO knee are from Ossur, Iceland; 3R106 PRO, 3R80, and 3R78 are from Ottobock, Germany; KX06 is from Endolite, India; Jiguang knee is from Zeanso, China.

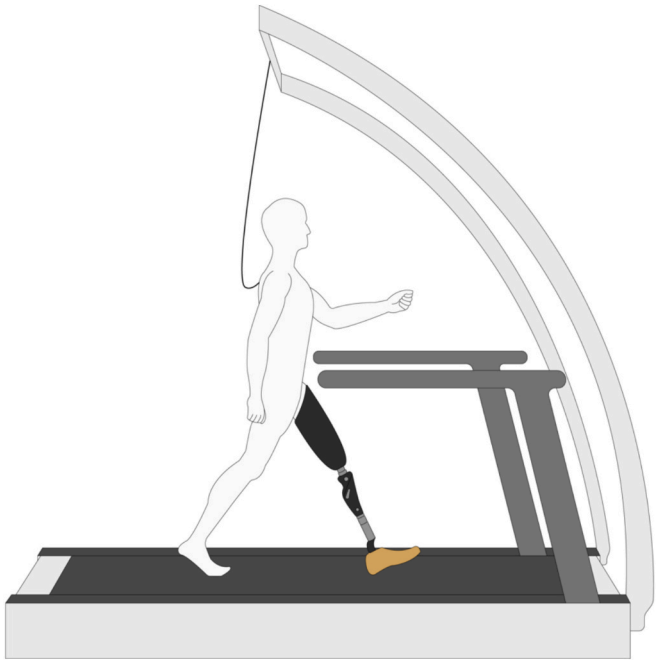

Fig. 1. Illustration of the experimental setting. Participants walked on a treadmill at their self-selected walking speed, secured by safety belt.

speed until participants confirmed that it felt comfortable and sustainable. They all wore their own shoes during walking to ensure that the alignment of their prostheses remained unchanged. The gait analysis FDM-T module (an operation mode of the Zebris FDM-T treadmill) was used to collect data. Adequate rest was given between the trials to minimize the effects of fatigue. All individuals wore a safety harness during walking, which was set to an appropriate tension to ensure it would not interfere with the walking (Fig. 1).

2.3. Data analyses

2.3.1. Spatiotemporal and vGRF parameters

All data were processed utilizing the Zebris FDM software (Zebris Medical GmbH, Germany). vGRF was recorded via pressure sensors embedded underneath the treadmill belt at a sampling rate of 300 Hz and used to identify specific gait phases. Both the duration time (in seconds) and percentage of the gait cycle were obtained for both sides. The first and second peaks of the vGRF were detected using a custom Python script, defined as the maximum values within the first 50 % and last 50 % of the gait cycle, respectively. The processed vGRF output for the control, intact, and prosthetic limbs are presented in Supplementary Fig. 1, with each curve representing one participant. Additional spatiotemporal parameters including step length, stride length, step time of each side, stride time, cadence, step width, foot rotation, and total contact time were also collected by the treadmill. All parameters were defined and automatically calculated by the treadmill's built-in software. The average values of all parameters across the two trials were calculated for inclusion in subsequent parameter calculations or statistical analyses.

2.3.2. Absolute symmetry index (ASI)

Absolute symmetry indices were computed for defined gait parameters, including the first and second vGRF peaks, foot rotation, step length, step time and the percentage duration of each gait cycle. The ASI was calculated using equation (1) (Finco et al., 2023), where *IL* represents the parameters of the intact limb, *PL* represents the parameters of the prosthetic limb. Values of ASI closer to 0 % represent a higher level of symmetry, and further away from 0 % indicate a lower level of symmetry. All the features were then normalized within 0–1 by using the min–max normalization (equation (2), where i indicated each sample (Patro and Sahu, 2015).

$$ASI = \left| \frac{IL - PL}{0.5^{*}(IL + PL)} {}^{*}100\% \right| \tag{1}$$

$$ASI_i{}' = \frac{ASI_i - \min\ (ASI)}{\max\ (ASI) - \min\ (ASI)} \tag{2}$$

2.3.3. Model training for random forest

The feature matrix for 12 uTFA individuals and 12 non-disabled individuals was obtained (Table 2), and the dataset was split into training and test sets (10 uTFA individuals and 10 non-disabled individuals for training, and 2 uTFA individuals and 2 non-disabled individuals for testing). A random state was set to 62 to ensure consistent results across repeated runs and facilitate reproducibility. Subsequently, the random forest model training was conducted, constructing a total of 1000 estimators with a fixed random state of 62 to identify the importance of features that can differentiate individuals with uTFA from non-disabled.

Feature importance was then computed by the random forest model. The Gini Impurity was calculated using equation (3), where m indicates the number of samples and p_i the probability of sample i. The Total Impurity Decrease was calculated using equations (4), (5), and (6), where k represents the total number of child nodes in decision tree, N_{child_i} denotes the number of samples in the i^{th} child node, N_{parent} stands for the number of samples in the parent node, and T represents the total number of trees in the random forest model. For each feature j, its importance was determined as the cumulative impurity decrease divided by the sum of cumulative impurity decrease for all features (equation (7), with N representing the total number of features. The random forest model training was carried out using an open-source scikit-learn code (Version 1.3.2, available at https://scikit-learn.org/) in Python (Version 3.11).

$$Gini\ \ Impurity = 1 - \sum_{i=1}^{m} p_i^2 \tag{3}$$

$$Weighted\ \ avg = \sum_{i=1}^{k} \left(\frac{N_{child_i}}{N_{parent}} \times Gini(child_i) \right) \tag{4}$$

$$Impurity\ \ Decrease = Gini(parent) - Weighted\ \ avg \tag{5}$$

$$Total\ Impurity\ Decrease_j = \sum_{t=1}^{T} \sum_{nodesoft} Impurity\ Decrease_{j,t} \tag{6}$$

$$Importance_j = \frac{Total\ \ Impurity\ \ Decrease_j}{\sum_{k=1}^{N} Total\ \ Impurity\ \ Decrease_k} \tag{7}$$

To confirm the feature importance obtained from the random forest model, Maximum Relative Minimum Redundancy (MRMR) analysis was conducted. Each feature received an MRMR score, calculated using equation (8), where C represents the binary class label (0 = non-disabled individual, 1 = individual with uTFA), $I(X;Y)$ denotes the mutual information between two random variables, the second term captures the average redundancy of f with respect to all other features s, and $\alpha \in [0,1]$ is defined weight that balances relevance and redundancy.

$$MRMRscore = \alpha I(f;C) - (1-\alpha) \frac{1}{|F|-1} \sum_{s \in F, s \neq f} I(f;s) \tag{8}$$

2.3.4. Model training for k-means clustering

The feature matrix of 12 uTFA individuals was employed for k-means clustering (Table 2). The optimal number of clusters was determined using the following two evaluation methods: 1) the Silhouette Score, which measures cohesion within clusters and separation between clusters. The optimal number of clusters corresponds to the global maximum of this score, where cohesion is highest and clusters are most distinct;

Table 2
Parameter summary for feature selection and statistical testing.

Parameters	Units	Abbreviations	Random forest features	K-means features	Statistical test
(a) Demographic parameters					
Walking speed	km/h	WS	Y	Y	Y
Age	year	—	N	N	Y
Time since amputation	year	—	N	N	Y
Body height	m	—	N	N	Y
Body mass	kg	—	N	N	Y
BMI	kg/m^2	—	N	N	Y
Residual limb length	cm	—	N	N	Y
(b) Spatiotemporal parameters					
Double limb support duration time	%	DLS	Y	Y	Y
Stride time	s	SDT	Y	Y	Y
Cadence	steps/min	—	Y	Y	Y
Stride length	cm	SDL	Y	Y	Y
Step width	cm	SPW	Y	Y	Y
Total contact time	s	TC	Y	Y	N
Stance phase duration time of prosthetic limb	s	STA PL	N	N	Y
Stance phase duration time of intact limb	s	STA IL	N	N	Y
Loading response duration time of prosthetic limb	s	LR PL	N	N	Y
Loading response duration time of intact limb	s	LR IL	N	N	Y
Single limb support duration time of prosthetic limb	s	SLS PL	N	N	Y
Single limb support duration time of intact limb	s	SLS IL	N	N	Y
Pre-swing duration time of prosthetic limb	s	PS PL	N	N	Y
Pre-swing duration time of intact limb	s	PS IL	N	N	Y
Swing phase duration time of prosthetic limb	s	SW PL	N	N	Y
Swing phase duration time of intact limb	s	SW IL	N	N	Y
Double limb support duration time	s	DLS	N	N	Y
Stance phase duration time of prosthetic limb	%	STA PL	N	N	Y
Stance phase duration time of intact limb	%	STA IL	N	N	Y
Loading response duration time of prosthetic limb	%	LR PL	N	N	Y
Loading response duration time of intact limb	%	LR IL	N	N	Y
Single limb support duration time of prosthetic limb	%	SLS PL	N	N	Y
Single limb support duration time of intact limb	%	SLS IL	N	N	Y
Pre-swing duration time of prosthetic limb	%	PS PL	N	N	Y
Pre-swing duration time of intact limb	%	PS IL	N	N	Y
Swing phase duration time of prosthetic limb	%	SW PL	N	N	Y
Swing phase duration time of intact limb	%	SW IL	N	N	Y
Step time of prosthetic limb	s	SPT PL	N	N	Y
Step time of intact limb	s	SPT IL	N	N	Y
Step length of prosthetic limb	cm	SPL PL	N	N	Y
Step length of intact limb	cm	SPL IL	N	N	Y
First peak of vGRF of prosthetic limb	%BM	FP PL	N	N	Y
First peak of vGRF of intact limb	%BM	FP IL	N	N	Y
Second peak of vGRF of prosthetic limb	%BM	SP PL	N	N	Y
Second peak of vGRF of intact limb	%BM	SP IL	N	N	Y
Foot rotation	°	—	N	N	N
(c) ASI parameters					
Absolute symmetry index of loading response	%	ASI LR	Y	Y	Y
Absolute symmetry index of single limb support	%	ASI SLS	Y	Y	Y
Absolute symmetry index of pre-swing	%	ASI PS	Y	Y	Y
Absolute symmetry index of swing phase	%	ASI SW	Y	Y	Y
Absolute symmetry index of step length	%	ASI SPL	Y	Y	Y
Absolute symmetry index of step time	%	ASI SPT	Y	Y	Y
Absolute symmetry index of first peak	%	ASI FP	Y	Y	Y
Absolute symmetry index of second peak	%	ASI SP	Y	Y	Y
Absolute symmetry index of foot rotation	%	ASI FR	Y	Y	N
Absolute symmetry index of stance phase	%	ASI STA	N	N	Y

Abbreviations: BMI: body mass index; BM: body mass; ASI: absolute symmetry index; Y: yes; N: no.
Note: The parameters between the double lines in demographic, spatiotemporal, and ASI parameters were used for model training.

and 2) the Elbow Method, which identifies the optimal number of clusters by finding the 'elbow' point where adding additional clusters no longer significantly reduces variation (Shahapure and Nicholas, 2020; Thorndike, 1953). To visualize the distribution of samples in two-dimensional space, dimensionality reduction using principal components analysis (PCA) was performed to capture the main variance in the dataset (Jolliffe, 2002). PCA was used exclusively for visualization, projecting the high-dimensional feature space onto two principal components for a clear display of the k-means clustering results. It was not used as input for the clustering algorithm or included in any subsequent statistical analyses. The overall data processing flowchart is illustrated in **Supplementary Fig. 2**.

2.4. Statistics

After determining the optimal number of clusters using the Silhouette Score and Elbow Method, statistical comparisons were conducted among the identified clusters with respect to demographic (Table 2 **(a)**), spatiotemporal (Table 2 **(b)**), and ASI parameters (Table 2 **(c)**) to test the hypothesis. The Shapiro-Wilk test was used to assess the normality of the data. A one-way analysis of variance (ANOVA) was used for normally distributed data to find differences among the three clusters, with subsequent application of Tukey's post hoc test to correct for multiple comparisons. The independent-samples Kruskal-Wallis's test was used to detect potential differences among the three clusters for the data of non-normal distribution. The significance threshold was set at alpha (α) = 0.05, and all the analyses for discrete parameters were conducted using SPSS (IBM SPSS Statistics 26, SPSS Inc., Chicago, IL).

3. Results

3.1. Demographic parameters' difference among clusters

No significant demographic differences were found among clusters (Table 3).

3.2. Feature importance and clustering results

The primary objective was to measure feature importance in distinguishing individuals with uTFA from able-bodied controls using a random forest model. The model, assessed by cross-validation (Cross-validation = 5), achieved 100 % accuracy. Feature importance results (Fig. 2**c**) ranked the parameters as follows: ASI SW (24.4 %), ASI SLS (21.4 %), ASI SPT (13.6 %), ASI FP (7.7 %), ASI LR (5.7 %), ASI PS (5.6 %), SPW (5.4 %), WS (4.6 %), SDT (2.8 %), cadence (2.1 %), TC (2.1 %), ASI SP (1.5 %), ASI SPL (1.4 %), SDL (0.6 %), ASI FR (0.6 %), and DLS (0.3 %). Clustering analysis identified three optimal clusters based on the Silhouette Score and Elbow Method (Figs. 2**a, 2b**). Fig. 2**d** shows the distribution of the cluster 1 (C1), cluster 2 (C2), and cluster 3 (C3). C1 included participant 1–4; C2 included participant 5–8; and C3 included participant 9–12. MRMR analysis ranked the features as follows: ASI SLS (0.579), ASI SW (0.484), ASI SPT (0.462), WS (0.379), ASI LR (0.212), ASI SP (0.203), ASI PS (0.195), SPW (0.192), ASI FP (0.174), cadence (0.137), ASI SPL (0.122), TC (0.121), SDT (0.110), ASI FR (0.068), DLS (−0.001), and SDL (−0.002) (Fig. 3).

3.3. Spatiotemporal and ASI parameters' differences among clusters

The second objective and hypothesis aimed to determine whether clustering would reveal distinct gait patterns with significant differences in spatiotemporal and symmetry parameters. Significant differences in spatiotemporal parameters were found: C3 exhibited significantly lower STA IL (s) ($p = 0.02$, Cohen's $d = 3.49$), lower LR PL (s) ($p = 0.05$, Cohen's $d = 2.36$), lower PS IL (s) ($p = 0.05$, Cohen's $d = 2.36$), lower DLS (s) ($p = 0.04$, Cohen's $d = 2.55$), and higher cadence ($p = 0.03$, Cohen's $d = 4.04$) compared to C1; C3 exhibited significantly lower SPL IL ($p = 0.02$, Cohen's $d = 2.56$) and lower SDL ($p = 0.01$, Cohen's $d = 2.84$) compared to C2; C3 showed significantly lower SPT PL than both C1 ($p = 0.02$, Cohen's $d = 3.33$) and C2 ($p = 0.04$, Cohen's $d = 2.02$); C1 exhibited significantly higher STA IL (%) ($p = 0.03$, Cohen's $d = 3.49$), lower SLS PL (%) ($p = 0.03$, Cohen's $d = 3.47$), and lower SW IL (%) ($p = 0.03$, Cohen's $d = 3.49$) compared to C2 (Table 4). Significant differences in ASI parameters were also observed: C2 exhibited significantly lower ASI STA ($p = 0.01$, Cohen's $d = 2.56$), lower ASI SLS ($p = 0.01$, Cohen's $d = 3.41$), and lower ASI SW ($p < 0.01$, Cohen's $d = 3.35$) compared to C1 while C1 showed significantly higher ASI SPL than both C2 ($p < 0.01$, Cohen's $d = 3.52$) and C3 ($p = 0.02$, Cohen's $d = 2.07$) (Table 5).

Table 3
Demographic parameters of three clusters.

Parameters	C1	C2	C3	p-value
Age (year)	51 ± 5	58 ± 7	52 ± 6	0.35
Time since amputation (year)	13.5 ± 11.8	33.0 ± 17.7	8.0 ± 3.5	0.15
Body height (m)	1.78 ± 0.04	1.76 ± 0.04	1.68 ± 0.09	0.21
Body mass (kg)	85.5 ± 11.5	67.3 ± 2.5	70.5 ± 19.5	0.25
BMI (kg/m^2)	27.3 ± 4.7	21.8 ± 1.3	24.5 ± 4.5	0.33
Residual limb length (cm)	21.8 ± 4.8	22.5 ± 4.8	21.8 ± 6.0	0.99
Walking speed (km/h)	1.53 ± 0.23	2.09 ± 0.43	1.75 ± 0.22	0.13

Abbreviations: C1: cluster 1; C2: cluster 2; C3: cluster 3; BMI: body mass index.

4. Discussion

In this study, the random forest algorithm was first employed to determine the importance of different symmetry parameters. Then, the k-means clustering algorithm was applied utilizing these parameters to identify three distinct clusters among individuals with uTFA.

The full feature set was used to train the clustering model for the following reasons: 1) when computational resources permit, using a larger set of features can improve model performance. Given the study's modest dataset and manageable computational demands, we opted to retain all features, and 2) clustering was also attempted using the top 2, 4, and 6 most important features identified by the random forest model. However, these reduced feature sets resulted in unstable centroids and low silhouette scores and thus failed to generate meaningful clusters. Given the limited sample size, dimensionality reduction based solely on feature importance was not effective in this case.

The first hypothesis was supported as the random forest model successfully identified the importance of all parameters for classification. Notably, cadence and step length, commonly used in previous clustering studies (Ichimura et al., 2022; Xu et al., 2006), exhibited low importance (cadence = 2.1 %, SPL = 1.4 %). In contrast, the duration time symmetry of the swing phase and single limb support emerged as highly influential (ASI SW = 24.4 %, ASI SLS = 21.4 %). To ensure that the variables highlighted by the random forest model were not artefacts of tree-based impurity metrics, we computed MRMR scores for all 16 input features. The top two features identified ASI SLS (MRMR score = 0.579) and ASI SW (MRMR score = 0.484), aligned with the random forest ranking. This convergence of two independent feature selection approaches confirms their significance for differentiating gait patterns in individuals with uTFA. It is worth mentioning that these two phases are essentially identical when considering duration time (Jacquelin Perry, 2010). However, the significance of single limb support cannot be overstated as individuals with uTFA tend to minimize weight-bearing on their prosthetic side, leading to shortened single limb support (Schmid et al., 2005). This temporal asymmetry is a hallmark of prosthetic gait symmetry.

It should be noted that the feature importance scores in this study were obtained by comparing uTFA gait with able-bodied gait, which may highlight ASI variables. However, this emphasis should not be viewed as a limitation. On the contrary, the prominent ranking of the ASI metrics reinforces the long-sanding clinical observation that bilateral asymmetry is a key distinguishing feature of uTFA gait (Agrawal et al., 2013; Cutti et al., 2018; Highsmith et al., 2016). This focus on asymmetry establishes a meaningful reference point for the overall deviation between these two populations, an 'outer layer' against which finer, within-group variations such as cadence or step length can be interpreted. Essentially, the ASI variables quantify the extent to which an individual departs from typical gait symmetry, whereas the spatiotemporal variables characterize how that departure manifests in terms of movement metrics. Although ASI parameters may show limited

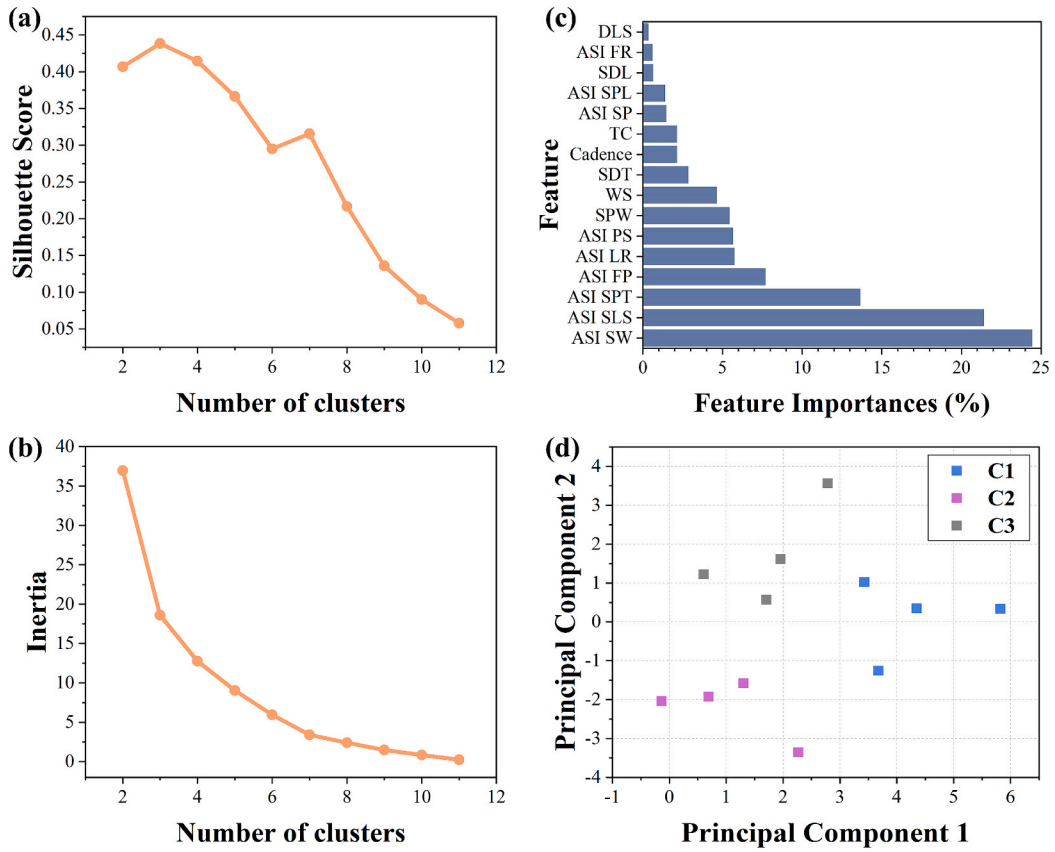

Fig. 2. K-means cluster results and features importance. (a) is the result of Silhouette Score, (b) shows the elbow method. (c) is the results of feature importance, ASI: absolute symmetry index; SW: swing phase; SLS: single limb support; SPT: step time; FP: first peak; LR: loading response; PS: pre-swing; SPW: step width; WS: walking speed; SDT: stride time; TC: total contact time; SP: second peak; SPL: step length; SDL: stride length; FR: foot rotation; DLS: double limb support. (d) shows the samples distribution after conducting principal component analysis (PCA) of all the features and the results of k-means cluster (k = 3).

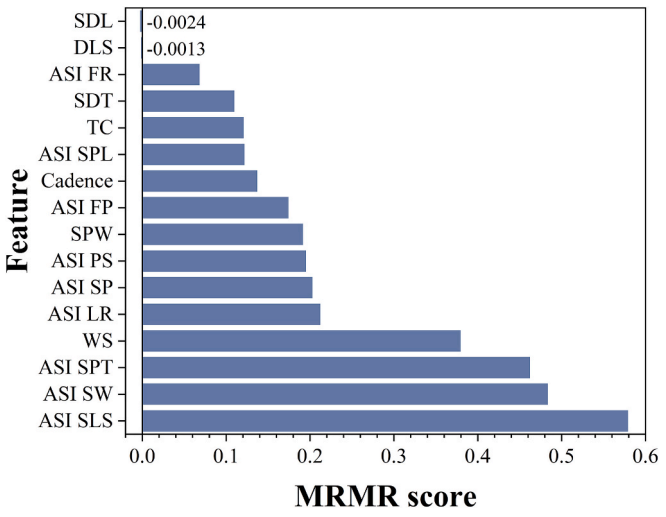

Fig. 3. Maximum-relevance-minimum-redundancy (MRMR) ranking of all 16 input features. Bars show the MRMR score assigned to each feature, ordered from highest (bottom) to lowest (top). ASI: absolute symmetry index; SLS: single limb support; SW: swing phase; SPT: step time; WS: walking speed; LR: loading response; SP: second peak; PS: pre-swing; SPW: step width; FP: first peak; SPL: step length; TC: total contact time; SDT: stride time; FR: foot rotation; DLS: double limb support; SDL: stride length.

variability within the individuals with uTFA, the random forest results suggest that they are among the most informative features for distinguishing gait patterns and may represent the most promising targets for functional improvement.

The second hypothesis was supported as there were significant differences in spatiotemporal and symmetry parameters among the three distinct clusters of individuals with uTFA. These clusters exhibited diverse gait patterns, with C1 displaying the lowest symmetry and the shortest duration time of the single limb support on the prosthetic limb, C2 demonstrating the highest symmetry and the longest bilateral stride length, and C3 featuring the highest cadence. Training focused on increasing step length and extending the duration time of the single limb support on the prosthetic limb could potentially enhance gait symmetry (C1 vs. C2). The extended single limb support allows for a longer stride length, and relies on the strength of the hip muscle groups (Wentink et al., 2013). For individuals in C1, targeted training to increase step length and extend the duration of single limb support on the prosthetic limb—such as by strengthening hip abductors and extensors—may help improve balance and confidence in weight-bearing (Wakasa et al., 2010). However, the influence of cadence on gait symmetry remains inconclusive when comparing C2 and C3. While C3 exhibited more asymmetry compared to C2, the difference did not reach statistical significance. For individuals in C3, who already have high cadence but exhibit asymmetry, interventions aimed at modulating cadence and increasing stride length may help enhance stability and improve overall gait symmetry by reducing reliance on high cadence alone.

In practice, gait symmetry is influenced by numerous factors, many of which may contribute to an increased step length. Achieving a relatively longer step length on the intact side often depends on a sufficient duration of single limb support on the prosthetic side, which requires

Table 4
Mean value, SD value, normality, p-value, and post-hoc analysis of spatiotemporal and vGRF parameters.

Parameters	Clusters			p-value (main effect)	Post-hoc		
	C1	C2	C3		C1-C2	C1-C3	C2-C3
STA PL (s)	1.01 ± 0.07	1.00 ± 0.17	0.77 ± 0.03	**0.04***	0.98	0.05	0.07
STA IL (s)	1.23 ± 0.11	1.10 ± 0.17	0.90 ± 0.03	**0.02***	0.44	**0.02***	0.13
LR PL (s)	0.37 ± 0.04	0.28 ± 0.06	0.25 ± 0.04	0.05	0.15	**0.05***	0.75
LR IL (s)	0.28 ± 0.04	0.27 ± 0.05	0.20 ± 0.02	0.07	—	—	—
SLS PL (s)	0.36 ± 0.03	0.45 ± 0.08	0.32 ± 0.05	0.05	—	—	—
SLS IL (s)	0.58 ± 0.06	0.56 ± 0.09	0.45 ± 0.04	0.11	—	—	—
PS PL (s)	0.28 ± 0.04	0.27 ± 0.05	0.20 ± 0.02	0.07	—	—	—
PS IL (s)	0.37 ± 0.04	0.28 ± 0.06	0.25 ± 0.04	0.05	0.15	**0.05***	0.75
SW PL (s)	0.58 ± 0.06	0.56 ± 0.09	0.45 ± 0.04	0.11	—	—	—
SW IL (s)	0.36 ± 0.03	0.45 ± 0.08	0.32 ± 0.05	0.05	—	—	—
DLS (s)	0.65 ± 0.06	0.55 ± 0.10	0.45 ± 0.06	**0.04***	0.36	**0.04***	0.32
STA PL (%)	63.7 ± 1.8	64.1 ± 2.6	63.3 ± 2.8	0.92	—	—	—
STA IL (%)	77.3 ± 1.7	71.3 ± 1.3	74.0 ± 3.6	**0.04***	**0.03***	0.26	0.39
LR PL (%)	23.4 ± 0.6	18.1 ± 1.7	20.9 ± 4.1	0.09	—	—	—
LR IL (%)	17.6 ± 2.3	17.3 ± 2.8	16.4 ± 2.3	0.82	—	—	—
SLS PL (%)	22.7 ± 1.7	28.7 ± 1.3	26.0 ± 3.5	**0.04***	**0.03***	0.25	0.38
SLS IL (%)	36.3 ± 1.8	35.9 ± 2.6	36.7 ± 2.8	0.92	—	—	—
PS PL (%)	17.6 ± 2.3	17.3 ± 2.8	16.4 ± 2.3	0.82	—	—	—
PS IL (%)	23.4 ± 0.6	18.1 ± 1.7	20.9 ± 4.1	0.09	—	—	—
SW PL (%)	36.3 ± 1.9	35.9 ± 2.6	36.7 ± 2.9	0.92	—	—	—
SW IL (%)	22.7 ± 1.7	28.8 ± 1.3	26.0 ± 3.6	**0.04***	**0.03***	0.25	0.38
DLS (%)	41.0 ± 2.8	35.3 ± 3.8	37.3 ± 6.2	0.34	—	—	—
SPT PL (s)	0.85 ± 0.08	0.82 ± 0.11	0.65 ± 0.02	**0.02***	0.84	**0.02***	**0.04***
SPT IL (s)	0.73 ± 0.06	0.73 ± 0.14	0.57 ± 0.02	0.09	—	—	—
SDT (s)	1.58 ± 0.13	1.55 ± 0.25	1.22 ± 0.04	**0.04***	0.97	0.05	0.08
Cadence (steps/min)	76 ± 6	80 ± 14	99 ± 3	**0.03***	0.89	**0.03***	0.06
SPL PL (cm)	29.8 ± 8.5	44.9 ± 3.6	28.9 ± 6.4	0.06	—	—	—
SPL IL (cm)	37.0 ± 4.7	42.6 ± 4.6	30.6 ± 3.5	**0.02***	0.30	0.21	**0.02***
SDL (cm)	66.9 ± 10.3	87.6 ± 8.0	59.5 ± 9.2	**0.01***	0.05	0.60	**0.01***
SPW (cm)	21.3 ± 4.8	14.7 ± 0.5	21.8 ± 5.1	0.12	—	—	—
FP PL (%BM)	88.4 ± 20.5	71.9 ± 9.9	69.0 ± 14.1	0.30	—	—	—
FP IL (%BM)	61.5 ± 5.5	62.4 ± 6.5	69.0 ± 13.8	0.58	—	—	—
SP PL (%BM)	74.4 ± 12.4	76.4 ± 13.6	87.7 ± 13.0	0.44	—	—	—
SP IL (%BM)	74.5 ± 14.1	82.0 ± 13.1	87.2 ± 8.7	0.47	—	—	—

Abbreviations: C1: cluster 1; C2: cluster 2; C3: cluster 3; PL: prosthetic limb; IL: intact limb; C1-C2: post-hoc between cluster 1 and cluster 2; C1-C3: post-hoc between cluster 1 and cluster 3; C2-C3: post-hoc between cluster 2 and cluster 3; STA: stance; LR: loading response; SLS: single limb support; PS: pre-swing; SW: swing phase; DLS: double limb support; SPT: step time; SDT: stride time; SPL: step length; SDL: stride length; SPW: step width; FP: first peak; SP: second peak; BM: body mass. An asterisk (*) indicates a significant difference with $p < 0.05$.

Table 5
Mean value, SD value, normality, p-value, and post-hoc analysis of absolute symmetry index parameters.

Parameters (%)	Clusters			p-value (main effect)	Post-hoc		
	C1	C2	C3		C1-C2	C1-C3	C2-C3
ASI STA	19.4 ± 3.1	10.7 ± 2.8	15.7 ± 2.2	**0.01***	**0.01***	0.27	0.12
ASI LR	28.6 ± 11.5	12.9 ± 11.7	23.2 ± 8.8	0.25	—	—	—
ASI SLS	46.4 ± 7.5	21.9 ± 4.5	34.8 ± 7.7	**0.01***	**<0.01***	0.19	0.13
ASI PS	28.6 ± 11.5	12.9 ± 11.7	23.2 ± 8.8	0.25	—	—	—
ASI SW	46.3 ± 7.7	21.9 ± 4.6	34.8 ± 7.7	**0.01***	**<0.01***	0.15	0.10
ASI SPL	34.2 ± 8.8	6.6 ± 3.8	14.5 ± 7.7	**<0.01***	**<0.01***	**0.02***	0.40
ASI SPT	15.8 ± 4.8	12.7 ± 6.8	12.5 ± 2.4	0.67	—	—	—
ASI FP	33.3 ± 22.8	23.8 ± 12.2	22.1 ± 15.1	0.70	—	—	—
ASI SP	10.3 ± 6.3	7.5 ± 5.6	11.3 ± 3.2	0.65	—	—	—

Abbreviations: C1: cluster 1; C2: cluster 2; C3: cluster 3; PL: prosthetic limb; IL: intact limb; C1-C2: post-hoc between cluster 1 and cluster 2; C1-C3: post-hoc between cluster 1 and cluster 3; C2-C3: post-hoc between cluster 2 and cluster 3; ASI: absolute symmetry index; STA: stance; LR: loading response; SLS: single limb support; PS: pre-swing; SW: swing phase; SPL: step length; SPT: step time; FP: first peak; SP: second peak. An asterisk (*) indicates a significant difference with $p < 0.05$.

strong support and stability—conditions associated with well-developed hip musculature on the prosthetic side. Strengthening the hip muscles benefits all individuals with uTFA (Riley et al., 2007), although the intensity of training may vary. For instance, C1 represents the gait pattern

most in need of hip muscle strengthening, while C3, where symmetry is relatively better, may benefit more from cadence adjustment.

Although changes in double limb support phase in the gait of individuals with uTFA have been widely recognized in rehabilitation settings (He et al., 2024), our study is the first to show that asymmetry and spatiotemporal measures can be used to classify individuals with uTFA into three reproducible clusters, each showing a distinct gait pattern. The inherent complexity of uTFA gait makes traditional classification approaches insufficient (Harandi et al., 2020; Heitzmann et al., 2020). Our findings offer a clinically meaningful framework for establishing a more consistent gait taxonomy that can support personalized rehabilitation strategies. From a broader clinical perspective, these insights are valuable. For example, in individuals assigned to C1 or C3, therapists could prioritize addressing major asymmetries such as unequal single limb support phase or swing phase duration before fine-tuning cadence or other secondary gait mechanics. Furthermore, the identified clusters can inform clinical decisions regarding prosthetic alignment and component selection. For instance, individuals exhibiting reduced single limb support duration might benefit from enhanced knee stability settings, while those with high cadence and short step length could improve their gait by increasing the initial flexion angle of the socket to enhance hip extension during terminal stance or by incorporating dynamic response foot components.

Our findings both confirm and extends the results of a previous clustering study (Ichimura et al., 2022). Similar to their hierarchical approach, our methods identified three distinct gait clusters among individuals with uTFA, reinforcing the notion that uTFA gaits is not a single, homogeneous pattern. However, the studies differ in the variables driving cluster formation and consequently in their clinical implications. In the previous study (Ichimura et al., 2022), clustering was based on cadence and step length data collected across eight fixed treadmill speeds, with cluster structure influenced primarily by participant body size and prosthetic knee components. In contrast, our study used sixteen features derived from symmetry indices and vGRF data collected at each participant's self-selected speed. Taken together, these two studies offer complementary insights: step length and cadence patterns capture how individuals with uTFA adapt across a range of walking speeds, whereas symmetry-based features show how much their gait deviates from bilateral norms at their preferred speed. Clinically, the cadence/step length-based clusters suggest tailoring interventions to anthropometric factors and prosthetic technology, whereas our symmetry-based clusters support a progressive rehabilitation pathway, first targeting fundamental gait asymmetries (especially the single limb support and swing phases), and then fine-tuning cadence and stride parameters to optimize functional performance.

The study has several limitations. First, the analysis of feature importance focused mainly on symmetry parameters derived from spatiotemporal and vGRF data. Future research should include a broader range of gait parameters, such as joint angles and moments, for a more comprehensive assessment. Second, all available features were employed in the clustering process without prioritization. The limited number of features could have led to an incomplete characterization of gait patterns. Further investigations should explore features selection strategies that consider varying levels of importance. Third, treadmill-based assessments may not fully capture overground gait characteristics, where environmental factors and natural walking patterns differ (Riley et al., 2007). Finally, the sample size was modest. Although previous clustering studies on individuals with uTFA typically enrolled 10–20 participants (Jamieson et al., 2023; Liu et al., 2022), larger cohorts would enable more robust cluster structures and finer distinctions among gait types. In this study, each cluster contained only four participants, so between-cluster comparisons should be considered exploratory and interpreted with caution. Furthermore, variability in prosthetic knee and foot components across participants may have amplified the limitations of the small sample size and potentially affect the clustering outcomes. Future research should aim to reduce component variability to enhance the reliability and generalizability of clustering outcomes.

In conclusion, this study highlights the importance of swing phase and single limb support duration symmetries as key features for distinguishing individuals with uTFA from non-disabled, as determined by the random forest algorithm. Subsequently, k-means clustering algorithm identified three distinct gait patterns among individuals with uTFA. These patterns are categorized as follows: C1, characterized by the lowest symmetry and shortest single limb support duration, could indicate a clinical need for interventions focusing on balance and weight acceptance; C2, exhibiting high symmetry and extended stance duration, aligns with stable gait patterns typically targeted for endurance and strength training; C3, with moderate symmetry but high cadence, suggests a focus on cadence modulation and gait stability. Customized rehabilitation training tailored to specific gait deviation patterns may better support individuals with uTFA in improving their gait performance.

CRediT authorship contribution statement

Yufan He: Writing – original draft, Software, Methodology, Investigation, Formal analysis, Data curation, Conceptualization. **Mingyu Hu:** Writing – review & editing, Methodology, Investigation, Data curation. **Alpha C.H. Lai:** Writing – review & editing, Investigation, Data curation. **Mark W.P. Koh:** Writing – review & editing, Investigation, Data curation. **Hiroaki Hobara:** Writing – review & editing, Methodology, Formal analysis. **Fan Gao:** Writing – review & editing, Methodology, Formal analysis. **Toshiki Kobayashi:** Writing – review & editing, Supervision, Project administration, Methodology, Investigation, Formal analysis, Conceptualization.

Declaration of competing interest

The authors declare that they have no known competing financial interests or personal relationships that could have appeared to influence the work reported in this paper.

Acknowledgements

This research received no external funding.

Appendix A. Supplementary data

Supplementary data to this article can be found online at https://doi.org/10.1016/j.jbiomech.2025.112920.

Data availability

Data will be made available on request.

References

Abbasi, L., Rojhani-Shirazi, Z., Razeghi, M., Raeisi-Shahraki, H., 2021. Kinematic cluster analysis of the crouch gait pattern in children with spastic diplegic cerebral palsy using sparse K-means method. Clin. Biomech. 81, 105248.

Agrawal, V., Gailey, R., O'Toole, C., Gaunaurd, I., Finnieston, A., 2013. Influence of gait training and prosthetic foot category on external work symmetry during unilateral transtibial amputee gait. Prosthet. Orthot. Int. 37, 396–403.

Bell, J.C., Wolf, E.J., Schnall, B.L., Tis, J.E., Tis, L.L., Potter, M.B.K., 2013. Transfemoral amputations: the effect of residual limb length and orientation on gait analysis outcome measures. JBJS 95, 408–414.

Chantraine, F., Schreiber, C., Pereira, J.A.C., Kaps, J., Dierick, F., 2022. Classification of stiff-knee gait kinematic severity after stroke using retrospective k-means clustering algorithm. J. Clin. Med. 11, 6270.

Cutti, A.G., Verni, G., Migliore, G.L., Amoresano, A., Raggi, M., 2018. Reference values for gait temporal and loading symmetry of lower-limb amputees can help in refocusing rehabilitation targets. J. Neuroeng. Rehabil. 15, 61.

Finco, M.G., Moudy, S.C., Patterson, R.M., 2023. Normalized kinematic walking symmetry data for individuals who use lower-limb prostheses: considerations for clinical practice and future research. J Prosthet Orthot 35, e1–e17.

Gjovaag, T., Starholm, I.M., Mirtaheri, P., Hegge, F.W., Skjetne, K., 2014. Assessment of aerobic capacity and walking economy of unilateral transfemoral amputees. Prosthet. Orthot. Int. 38, 140–147.
Harandi, V.J., Ackland, D.C., Haddara, R., Lizama, L.E.C., Graf, M., Galea, M.P., Lee, P.V. S., 2020. Gait compensatory mechanisms in unilateral transfemoral amputees. Med. Eng. Phys. 77, 95–106.
He, Y., Hu, M., Jor, A., Hobara, H., Gao, F., Kobayashi, T., 2024. Dynamics of Center of pressure trajectory in gait: unilateral transfemoral amputees versus non-disabled individuals. IEEE Trans. Neural Syst. Rehabilit. Eng.
Heitzmann, D.W.W., Leboucher, J., Block, J., Günther, M., Putz, C., Götze, M., Wolf, S.I., Alimusaj, M., 2020. The influence of hip muscle strength on gait in individuals with a unilateral transfemoral amputation. PLoS One 15, e0238093.
Highsmith, M.J., Andrews, C.R., Millman, C., Fuller, A., Kahle, J.T., Klenow, T.D., Lewis, K.L., Bradley, R.C., Orriola, J.J., 2016. Gait training interventions for lower extremity amputees: a systematic literature review. Technol. Innovat. 18, 99–113.
Ichimura, D., Amma, R., Hisano, G., Murata, H., Hobara, H., 2022. Spatiotemporal gait patterns in individuals with unilateral transfemoral amputation: a hierarchical cluster analysis. PLoS One 17, e0279593.
Jacquelin Perry, M., 2010. Gait analysis: normal and pathological function. SLACK, New Jersey.
Jamieson, A., Murray, L., Stankovic, V., Stankovic, L., Buis, A., 2023. Unsupervised cluster analysis of walking activity data for healthy individuals and individuals with lower limb amputation. Sensors 23, 8164.
Jolliffe, I.T., 2002. Graphical representation of data using principal components. Principal Component Anal. 78–110.
Kaufman, K.R., Frittoli, S., Frigo, C.A., 2012. Gait asymmetry of transfemoral amputees using mechanical and microprocessor-controlled prosthetic knees. Clin. Biomech. 27, 460–465.
Keklicek, H., Kirdi, E., Yalcin, A., Topuz, S., Ulger, O., Erbahceci, F., Sener, G., 2019. Comparison of gait variability and symmetry in trained individuals with transtibial and transfemoral limb loss. J. Orthop. Surg. 27, 2309499019832665.
Kobayashi, T., Orendurff, M.S., Boone, D.A., 2013. Effect of alignment changes on socket reaction moments during gait in transfemoral and knee-disarticulation prostheses: case series. J. Biomech. 46, 2539–2545.
Krajbich, J.I., Pinzur, M.S., Potter, B.K., Stevens, P.M., 2023. Atlas of amputations and limb deficiencies: surgical, prosthetic, and rehabilitation principles. Lippincott Williams & Wilkins.
Liu, X., Wei, Q., Ma, H., An, H., Liu, Y., 2022. Muscle selection using ICA clustering and phase variable method for transfemoral amputees estimation of lower limb joint angles. Machines 10, 944.
Luo, G., Zhu, Y., Wang, R., Tong, Y., Lu, W., Wang, H., 2020. Random forest-based classsification and analysis of hemiplegia gait using low-cost depth cameras. Med. Biol. Eng. Compu. 58, 373–382.
Mobarak, R., Mengarelli, A., Verdini, F., Fioretti, S., Burattini, L., Tigrini, A., 2024. Enhanced Gait Phases Recognition by EMG and Kinematics Information Fusion and a Minimal Recording Setup. Al-Khwarizmi Eng. J. 20, 86–93.
Nolan, L., Wit, A., Dudziñski, K., Lees, A., Lake, M., Wychowañski, M., 2003. Adjustments in gait symmetry with walking speed in trans-femoral and trans-tibial amputees. Gait Posture 17, 142–151.
Patro, S., Sahu, K.K., 2015. Normalization: A preprocessing stage. arXiv preprint arXiv: 1503.06462.
Petersen, A.O., Comins, J., Alkjær, T., 2010. Assessment of gait symmetry in transfemoral amputees using C-leg compared with 3R60 prosthetic knees. JPO: J. Prosthetics Orthotics 22, 106–112.
Ranz, E.C., Wilken, J.M., Gajewski, D.A., Neptune, R.R., 2017. The influence of limb alignment and transfemoral amputation technique on muscle capacity during gait. Comput. Methods Biomech. Biomed. Eng. 20, 1167–1174.
Reed, L.F., Urry, S.R., Wearing, S.C., 2013. Reliability of spatiotemporal and kinetic gait parameters determined by a new instrumented treadmill system. BMC Musculoskelet. Disord. 14, 1–10.
Riley, P.O., Paolini, G., Della Croce, U., Paylo, K.W., Kerrigan, D.C., 2007. A kinematic and kinetic comparison of overground and treadmill walking in healthy subjects. Gait Posture 26, 17–24.
Roche, N., Pradon, D., Cosson, J., Robertson, J., Marchiori, C., Zory, R., 2014. Categorization of gait patterns in adults with cerebral palsy: a clustering approach. Gait Posture 39, 235–240.
Rutkowska-Kucharska, A., Kowal, M., Winiarski, S., 2018. Relationship between asymmetry of gait and muscle torque in patients after unilateral transfemoral amputation. Appl. Bionics Biomech.
Schaarschmidt, M., Lipfert, S.W., Meier-Gratz, C., Scholle, H.-C., Seyfarth, A., 2012. Functional gait asymmetry of unilateral transfemoral amputees. Hum. Mov. Sci. 31, 907–917.
Schmid, M., Beltrami, G., Zambarbieri, D., Verni, G., 2005. Centre of pressure displacements in trans-femoral amputees during gait. Gait Posture 21, 255–262.
Shahapure, K.R., Nicholas, C., Year Cluster quality analysis using silhouette score. In 2020 IEEE 7th international conference on data science and advanced analytics (DSAA).
Thorndike, R.L., 1953. Who belongs in the family? Psychometrika 18, 267–276.
Tigrini, A., Mobarak, R., Mengarelli, A., Khushaba, R.N., Al-Timemy, A.H., Verdini, F., Gambi, E., Fioretti, S., Burattini, L., 2024. Phasor-based myoelectric synergy features: a fast hand-crafted feature extraction scheme for boosting performance in gait phase recognition. Sensors 24, 5828.
Traballesi, M., Delussu, A.S., Averna, T., Pellegrini, R., Paradisi, F., Brunelli, S., 2011. Energy cost of walking in transfemoral amputees: comparison between Marlo Anatomical Socket and Ischial Containment Socket. Gait Posture 34, 270–274.
Van Alsenoy, K., Thomson, A., Burnett, A., 2019. Reliability and validity of the Zebris FDM-THQ instrumented treadmill during running trials. Sports Biomech. 18, 501–514.
Viteckova, S., Kutilek, P., Svoboda, Z., Krupicka, R., Kauler, J., Szabo, Z., 2018. Gait symmetry measures: a review of current and prospective methods. Biomed. Signal Process. Control 42, 89–100.
Wakasa, M., Seki, K., Fukuda, A., Sasaki, K., Izumi, S.-I., 2010. Muscle activity and postural control during standing of healthy adults wearing a simulated trans-femoral prosthesis. J. Phys. Ther. Sci. 22, 233–238.
Wentink, E.C., Prinsen, E.C., Rietman, J.S., Veltink, P.H., 2013. Comparison of muscle activity patterns of transfemoral amputees and control subjects during walking. J. Neuroeng. Rehabil. 10, 1–11.
Winiarski, S., Rutkowska-Kucharska, A., Kowal, M., 2021. Symmetry function–an effective tool for evaluating the gait symmetry of trans-femoral amputees. Gait Posture 90, 9–15.
Xu, G., Zhang, Y., Begg, R., Year Mining gait pattern for clinical locomotion diagnosis based on clustering techniques. In Advanced Data Mining and Applications: Second International Conference, ADMA 2006, Xi'an, China, August 14-16, 2006 Proceedings 2.
Zeni Jr, J.A., Higginson, J.S., 2010. Gait parameters and stride-to-stride variability during familiarization to walking on a split-belt treadmill. Clin. Biomech. 25, 383–386.
Zhang, T., Bai, X., Liu, F., Fan, Y., 2019. Effect of prosthetic alignment on gait and biomechanical loading in individuals with transfemoral amputation: a preliminary study. Gait Posture 71, 219–226.